



Perturbative theory of statistically averaged atomic dynamics in fluctuating laser fieldsTejaswi Katravulapally  and L. A. A. Nikolopoulos **School of Physical Sciences, Dublin City University, Dublin 9, Ireland*

(Received 3 June 2020; accepted 28 October 2020; published 16 November 2020)

We have developed a perturbative method to model the resonant ionization of atomic systems in fluctuating laser fields. The perturbative method is based on an expansion in terms of the multitime cumulants, a suitable combination of moments (field's coherence functions), used to represent the field's statistical properties. The second-order truncated expansion is expressed in terms of the radiation's power spectrum and the intensity autocorrelation function. We investigate the range of validity of the model in terms of the field's coherence temporal length and peak intensity and have compared the results with conventional Monte Carlo calculations. We apply the theory in the case of a near-resonant ionization of the helium $2s2p$ autoionizing state with a self-amplified spontaneous emission free-electron laser pulse with square-exponentially dependent first-order coherence function. The ionization lineshape profile acquires a Voigt profile; the degree of the Gaussian or Lorentzian character of the lineshape will depend crucially on the field's coherence time.

DOI: [10.1103/PhysRevA.102.053111](https://doi.org/10.1103/PhysRevA.102.053111)**I. INTRODUCTION**

Following the advent of the free-electron laser (FEL) sources the dynamics of atomic systems under a randomly varying short-wavelength radiation has been a research area of interest for more than a decade now [1–3]. From a mathematical standpoint the field's randomness renders the system's equations-of-motion (EOMs) to a *stochastic differential equation* problem with the dynamical quantities treated as stochastic processes [4–6]. The practical problem faced is to describe the statistics of these dynamical quantities (excited population, ionization yield, electron kinetic angular spectrum, absorption spectrum, etc.) given the radiation's statistical properties. This typical probabilistic problem was dealt theoretically in detail in a very similar context soon after the first laser sources of long-wavelength radiation appeared and experimental data became available. The interested reader can find rigorous studies of these kinds of problems in the early works in the field and references therein [7–10]. With the later development of lasers with well-stabilized amplitude and phase (e.g., Ti:sapphire) the weakened fluctuations proved to play a negligible role in the excitation-ionization dynamics making a statistical description redundant. Nowadays, a quite similar scenario emerged for the FEL's radiation which exhibits strong temporal fluctuations, thus naturally triggering a revived interest about the effects of randomness in atomic photoionization dynamics [3,11–15]. A class of experimental schemes (multishot) measure data which have been generated over many pulses which differ from each other in a random manner; therefore, inevitably, these measurements provide the averaged values of the experimental observables. In mathematical parlance, they represent an ensemble average over the field's fluctuations. This simple fact brings to the forefront a

statistical description of the atomic dynamics. Therefore our main motivation is to perform a rigorous statistical average of the stochastic equations themselves; a deterministic set of equations-of-motion is obtained for the statistical average of the observable under question. The immediate benefit of the averaging process is a significant computational gain to calculate the desired averages; a second benefit is that although the averaged equations have a similar structure to their stochastic counterpart, usually it has kept only what is essential for the description of the interactions; eventually the system's dynamics EOMs are expressed in terms of directly accessible experimental quantities, for example, the autocorrelation spectrum, coherence time, and energy of the field [16].

More specifically, we present a systematic perturbation theory of near-resonant nonlinear photoionization via an autoionization state which takes into account the fluctuation statistics of the FEL radiation (Fig. 1). We assume the FEL pulses as described in the work by Krinsky and Li [17], which model the self-amplified spontaneous emission (SASE) start-up process as a shot-noise stochastic process [18–20]. According to this model, the first-order coherence function of the FEL radiation possesses a square-exponential (Gaussian) time dependence, $\sim e^{-(t_1-t_2)^2/2\tau_c^2}$ (this is distinctly different from the usually assumed, $\sim e^{-|t_1-t_2|/2\tau_c}$, of the early lasers of longer wavelength). The Gaussian-like dependence has been treated to date only within a Monte Carlo (MC) algorithm type of calculation [11,14]. One of the outcomes of the present formulation is the following: As usual, the infinite term perturbation series is exact, but, except for some simplified cases, one is led to truncate the perturbative expansion at a certain order; we have derived the physical conditions under which the truncation order is legitimate. As mentioned earlier the lowest-order term of the truncated expansion is expressed in terms of its temporal mean intensity and power spectrum; more accurately, the autocorrelation (AC) functions of the time-integrated electric field amplitude and intensity,

*lampros.nikolopoulos@dcu.ie

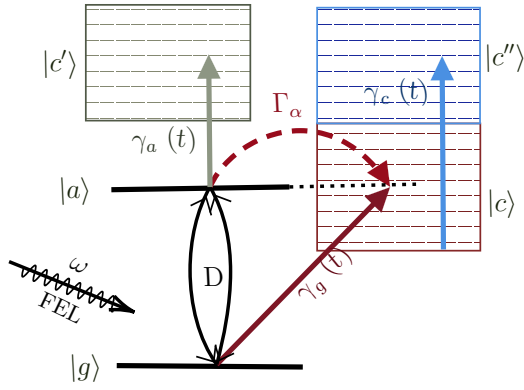


FIG. 1. Sketch of the excitation or ionization near-resonant scheme with a FEL pulse.

$\langle \mathcal{E}(t)\mathcal{E}^*(t') \rangle$ and $\langle \mathcal{I}(t)\mathcal{I}(t') \rangle$, respectively. It is worth noting here, that the intensity's coherence function is essential to be included because different random fields may share the same first AC function but not the second. This dependence of the dynamics on these AC functions becomes stronger for FEL fields obeying Gaussian statistics and especially at conditions where stationarity of the averages may be assumed (long pulses relative to the field's coherence time) [21]. Concluding with this general discussion the reader who is particularly interested in various standpoints of the theory of random processes could refer to related references [4,6,22–26]

The structure of the presentation is as follows: In Sec. II we start with a brief discourse on the EOM theory in stochastic fields followed by the detailed development of the particular perturbative method. In this section we arrive at an exact differential deterministic equation for the ensemble-averaged density matrix driven by a time-dependent perturbation expansion. The ionization scheme assumed is given in Fig. 1. We chose to develop the method using a Fano representation of the essential states for the reason that the experimental data are frequently and conveniently available in terms of the q -Fano parameter and the width of the autoionizing states. Apart from a “short” correlation-time requirement not any other particular assumption for the field is made. We also evaluate the first two nonvanishing terms of the series expansion and obtain Eqs. (29) and (37) for the bound and the singly ionized states of the system. These equations are the main result of this work. In Sec. III the terms of the truncated expansion are specialized for fields obeying Gaussian statistics for the cases where the first-order AC function decays as $\sim e^{-(t_1-t_2)^2/2\tau_c^2}$ and as $\sim e^{-|t_1-t_2|/2\tau_c}$; the former corresponds to the FEL radiation model mentioned earlier whereas the latter is more suitable for various models of long-wavelength laser radiation [27,28]. In Sec. IV we apply the method in the near-resonant ionization regime via the helium $2s2p$ autoionization state (~ 60.154 eV) for two FEL pulses, of different intensity full width at half maximum (FWHM) duration ~ 11.7 fs and 75 fs, and compare the results with a MC method.

In Conclusions we discuss limitations of the present method and further work along similar lines. Finally in the Appendix we have relegated some of the mathematical formulas outside the main text.

For the presentation of the formulas, atomic units are used throughout the text; For the reader's convenience other units (e.g., eV, fs) are used in the discussion section and the figure captions.

The less mathematically inclined reader may skip Sec. II altogether and focus on the more applied part of the text. The reader who is familiar with the theory of density-matrix resonant ionization and is mostly interested in the averaging method should focus on Sec. II B.

II. FORMULATION

Below we develop a perturbation method for the averaged density matrix equations which describes the excitation and ionization of an atomic system via an autoionizing state under a randomly fluctuating field. The discussion is kept general for any fluctuating radiation field, apart from the main assumption that the field's coherence time τ_c should be shorter than any other characteristic times relevant to the systems dynamics.

A. Resonant ionization density matrix equations

Assuming a Fano representation of the ionization scheme as in Fig. 1 [29–31], we define by $\rho(t)$ the atomic density matrix state and by $|g\rangle$, $|a\rangle$ the initial and the excited states with energies E_g and E_a , respectively. In addition, we denote the continuum states of the system, by $|c\rangle$, $|c'\rangle$, and $|c''\rangle$. The static part of the corresponding ionization widths, γ_g , γ_a , γ_c and the autoionization width Γ_a are defined in the following way: γ_g is associated with photoionization from the $|g\rangle$ in the $|c\rangle$ continuum, γ_a with photoionization from the resonant state $|a\rangle$ in the $|c'\rangle$ continuum states, while Γ_a represents the autoionization width from $|a\rangle$ in the $|c\rangle$ continuum. Finally $|c''\rangle$ represents the continuum states reached from the $|c\rangle$ states, following one-photon absorption; the associated static part of the ionization width is the γ_c . To clarify the notation even further we specialize this abstract Fano state in the case of the atomic helium. So, $|g\rangle$ is the helium ground state $|1s^2\rangle$, $|a\rangle$ corresponds to the bound part of the $|2s2p\ ^1P\rangle$ helium autoionization state, $|c\rangle$ corresponds to the $\text{He}^+(1s) + e^-$ continuum states, $|c'\rangle$ represents any state reached from $|a\rangle$ by one-photon transition while $|c''\rangle$ the doubly ionized helium states reached by ionization of the $\text{He}^+(1s)$ ground state.

Given the above clarifications, the density matrix elements of $\rho(t)$ are governed by the Liouville equation [32], $i\dot{\rho}(t) = [\hat{H}_a + \hat{V}(t), \rho(t)]$, where \hat{H}_a is the time-independent field-free atomic Hamiltonian operator and $\hat{V}(t)$ representing the random external potential. We take $\hat{V}(t) = -\hat{d}\mathcal{E}_R(t)$ to represent the electric dipole interaction with \hat{d} the atomic dipole operator. Following Mandel and Wolf [33] the external (linearly polarized) radiation field, $\mathcal{E}_R(t)$, can be modeled via a complex envelop, $\mathcal{E}(t) = \mathcal{E}_0(t)\epsilon(t)$ as

$$\mathcal{E}_R(t) = \text{Re}(\epsilon(t)\mathcal{E}_0(t)e^{i\omega t}). \quad (1)$$

$\mathcal{E}(t)$ is a complex random process, with the fluctuations modeled exclusively by the $\epsilon(t)$ complex random processes with $\langle |\epsilon(t)|^2 \rangle = 1$ where brackets denote the ensemble average over the field's fluctuations. By construction, the deterministic envelope $\mathcal{E}_0(t)$ is chosen such that the ensemble average of the

intensity envelope, $\mathcal{I}(t) = |\mathcal{E}(t)|^2$, is equal to [33,34]

$$\langle \mathcal{I}(t) \rangle = \langle |\mathcal{E}(t)|^2 \rangle = |\mathcal{E}_0(t)|^2. \quad (2)$$

Now, assume for a moment that no random fluctuations are present. For the near-resonant case the field-free evolution of the nondiagonal density matrix elements will vary sinusoidally as $(E_a - E_g)t \sim \omega t$, at the same time scale as the periodic part of the field. In the presence of the field a lot slower time variation on the density matrix elements of the system's state is superimposed $\sim |V_{ag}| \ll \omega$. We can take advantage of this difference and effectively remove the "fast" oscillating contribution. We then have to deal with the field's envelope slow temporal variation ($\sim \tau_p \gg 2\pi/\omega$). Apart from the $\sim 1/|V_{ag}|$ time scale the other characteristic time scales are determined by the autoionization decay rate $\sim 1/\Gamma_a$ and the maximum photoionization widths of the $|g\rangle$, $|a\rangle$, and $|c\rangle$ states. This is why it is convenient to use the field's envelope to develop a time-dependent perturbation theory.

With the field-free eigenvalue problem solved, the energies and the transition matrix element between the system's eigenstates can be calculated. Then we expand the density operator over its Hamiltonian eigenstate basis. As usual, the diagonal terms $\rho_{ii}(t)$, $i = g, a, c, c'$ provide the occupation probabilities for the system's eigenstates (*populations*) while the off-diagonal ones $i \neq j$, $\rho_{ij}(t)$, (atomic *coherences*) keep track of the phase relations among the various eigenstates. Next we keep only the states essential to the dynamics, by effective elimination of the off-resonant continuum states (those states which are off-resonant to $E_g + \omega$ and $E_a + \omega$). Briefly, we transform to a slowly varying representation with the diagonal elements left intact and the coherences changed by a phase factor, $\sigma_{ag} = \rho_{ag} e^{i(E_a - E_g)t}$ [35]. Following a standard procedure we arrive at a set of the density-matrix EOMs parametrized in terms of the slowly varying Rabi transition matrix element, ac-Stark shifts and ionization widths to the respective continua [36–38]:

$$\dot{\sigma}_{gg} = -\gamma_g \mathcal{I}(t) \sigma_{gg} + 2\text{Im}[\mathcal{D}\mathcal{E}(t)\sigma_{ag}], \quad (3a)$$

$$\dot{\sigma}_{aa} = -[\Gamma_a + \gamma_a \mathcal{I}(t)]\sigma_{aa} - 2\text{Im}[\mathcal{D}^* \mathcal{E}(t)\sigma_{ag}], \quad (3b)$$

$$\dot{\sigma}_{ag} = -[\delta + \Delta \mathcal{I}(t)]\sigma_{ag} + i\mathcal{D}^* \mathcal{E}^*(t)\sigma_{aa} - i\mathcal{D}\mathcal{E}^*(t)\sigma_{gg}, \quad (3c)$$

$$\dot{\sigma}_{cc} = -\gamma_c \mathcal{I}(t)\sigma_{cc} - \dot{\sigma}_{gg} - \dot{\sigma}_{aa}, \quad (3d)$$

$$\dot{\sigma}_{c'c'} = \gamma_a \mathcal{I}(t)\sigma_{aa}. \quad (3e)$$

$$L_b(t) = \begin{pmatrix} -\gamma_g \mathcal{I}(t) & 0 & -i\mathcal{E}(t)\mathcal{D} & i\mathcal{E}^*(t)\mathcal{D}^* \\ -\Gamma_a & -\gamma_a \mathcal{I}(t) & i\mathcal{E}(t)\mathcal{D}^* & -i\mathcal{E}^*(t)\mathcal{D} \\ -i\tilde{\mathcal{E}}^*(t)\mathcal{D} & i\mathcal{E}^*(t)\mathcal{D}^* & -(\delta + \Delta \mathcal{I}(t)) & 0 \\ i\mathcal{E}(t)\mathcal{D}^* & -i\mathcal{E}(t)\mathcal{D} & 0 & -(\delta + \Delta^*)\mathcal{I}(t) \end{pmatrix}, \quad (4)$$

with $L_b(t)$ temporally dependent on the fluctuating laser field envelope $\mathcal{E}(t)$ and its intensity $\mathcal{I}(t)$. At this point it is sufficient to say that we assume the field to have zero ensemble mean average $\langle \mathcal{E}(t) \rangle = 0$. It is beneficial to split the random dynamics into a deterministic part, represented by the ensemble average of the Liouville operator, $\bar{L}_b(t) \equiv \langle L_b(t) \rangle$, and a random term $\tilde{L}_b(t)$ with zero mean average, $\langle \tilde{L}_b(t) \rangle = 0$. This is done by splitting the intensity as $\mathcal{I}(t) = \langle \mathcal{I}(t) \rangle + \tilde{\mathcal{I}}(t)$ with,

For near-resonant laser frequencies the interatomic ionization channel, modeled by the Γ_a decay width, interferes with the direct photoionization channel from the $|g\rangle$ state (γ_g); the latter interference, strongly dependent on the laser and atomic particulars, is reflected in the experimental observables, e.g., ionization yield, photoelectron spectrum. Mathematically, this interference is represented in the dynamics equations by the complex Rabi transition matrix element \mathcal{D} and the complex peak detunings Δ, δ , the definitions of which are given in Appendix A.

Before proceeding to the main part of the present development we note that the first three equations which determine the bound-states dynamics are not directly coupled with the last two. The effect of the latter continua are represented by the associated ionization widths $\gamma_g, \gamma_a, \Gamma_a$ and ac-Stark shifts s_a, s_g . Generally this procedure, entailing a replacement of an effective density matrix with a nonconserved trace, is known as continuum elimination [35,37,39]. More specifically, the coupling with the continuum states is included indirectly in the ac-Stark shifts and the ionization widths but not directly with the continuum density matrix elements $\sigma_{cc}(t), \sigma_{c'c'}(t)$; so, effectively the continuum population dynamics does not affect the bound state's dynamics. On the other hand, asymmetrically, mere inspection of the remaining two equations for $\sigma_{cc}(t), \sigma_{c'c'}(t)$ shows that knowledge of the bound-state dynamics is essential. In our derivation below, we aim to follow a similar pattern, dictated from this remark: We'll be first dealing with the bound state dynamics exclusively, and then we'll be applying the developed method to the continuum part, as well.

B. Formal theory of averaging

The field's fluctuations introduce into the dynamics an additional aspect of the interaction between the field and the atomic system. The main parameters which characterize the fluctuations are their strength and coherence time τ_c ; the latter time, effectively, defines an extra characteristic dynamics time scale. The subject of this section is to develop a perturbative ensemble-averaging photoionization theory which takes properly into account these additional properties of the field.

We start by considering only the set of Eqs. (3a)–(3c) and write the bound part of the Liouville equation: $\dot{\sigma}_b(t) = L_b(t)\sigma(t)$ where $\sigma_b \equiv (\sigma_{gg}, \sigma_{aa}, \sigma_{ag}, \sigma_{ga})$ and

by construction, $\langle \tilde{\mathcal{I}}(t) \rangle = 0$. The bound part of the Liouville equation is now expressed by

$$\dot{\sigma}_b(t) = [\bar{L}_b(t) + \tilde{L}_b(t)]\sigma_b(t), \quad (5)$$

with initial conditions $\sigma_b(t_i) = (1, 0, 0, 0)$. The mean-averaged part is a diagonal matrix,

$$\bar{L}_b(t) = L_0 + L_2 \langle \mathcal{I}(t) \rangle, \quad (6)$$

while its random part is decomposed as

$$\tilde{L}_b(t) = L_1 \mathcal{E}(t) + L_1^T \mathcal{E}^*(t) + L_2 \tilde{\mathcal{I}}(t). \quad (7)$$

The explicit form of the 4×4 constant matrices, L_i , $i = 0 - 2$ and $\tilde{L}_b(t)$, is relegated in Appendix A. The above decomposition leads to a dynamics governed by noncommutative matrices, $[\tilde{L}_b(t), \tilde{L}_b(t')] \neq 0$, $([L_1, L_i] \neq 0, i = 0, 2$ but $[L_0, L_2] = 0)$. Another point to note is that although the initial time is introduced as t_i , at the end of the formal development it will be set to $t_i = -\infty$ (where the pulse is reasonably assumed negligible); this has the effect of rendering the averaged equations independent of the initial time t_i ; this is not just a practical matter but an essential step to turning properly a random differential equation to its averaged counterpart [4]. The derived averaged equations will be valid as long as a transient period of the time scale of few τ_c . The shortness of the coherence time entails to fast decaying coherence functions for the field ensuring any dependence (“memory”) on the initial time has been definitely lost, a natural consequence of the randomness of the process in the course of time.

Continuing with the formal steps of averaging Eq. (5) the deterministic part (mean average) of the dynamics is absorbed into a newly defined density matrix, through the transformation,

$$\sigma(t) = \bar{U}_b(t, t_i) \sigma_b(t), \quad (8)$$

$$\bar{U}_b(t, t_i) = e^{-\int_{t_i}^t d\tau' \tilde{L}_b(\tau')}, \quad (9)$$

with $\bar{U}_b(t, t_i)$ a deterministic evolution superoperator. Note that since \tilde{L}_b is diagonal this transformation does not require any specific chronological order to be prescribed. Also, it is worth mentioning here that $\langle U_b(t, t_i) \rangle \neq \bar{U}_b(t, t_i)$, albeit both sure functions of time. Performing the transformation of Eq. (8) in Eq. (5) the effective (interaction-picture) time evolution for the $\sigma(t)$ is

$$\dot{\sigma}(t) = \tilde{L}(t) \sigma(t), \quad \sigma(t_i) = \sigma_b(t_i), \quad (10)$$

with the stochastic interaction matrix $\tilde{L}(t)$ given by

$$\tilde{L}(t) = \bar{U}_b(t) \tilde{L}_b(t) \bar{U}_b^\dagger(t). \quad (11)$$

Given that $\bar{U}_b(t, t_i)$ is a deterministic evolution operator the mean value of the random interaction matrix $L(t)$ vanish as well:

$$\langle \tilde{L}(t) \rangle = \bar{U}_b(t) \langle \tilde{L}_b(t) \rangle \bar{U}_b^\dagger(t) = 0, \quad (12)$$

since by construction $\langle \tilde{L}_b(t) \rangle = 0$, as indicated earlier in the text. Temporarily, for convenience, the dependence on the initial time t_i is suppressed by setting $\bar{U}_b(t) \equiv \bar{U}_b(t, t_i)$. Equation (10) represents a typical multiplicative system of stochastic differential equations, heavily studied over the years in various contexts [4].

We chose to follow a perturbative approach by utilizing an infinite expansion solution of Eq. (10). The formal solution is given by

$$\sigma(t) = \tilde{U}(t) \sigma(t_i), \quad (13)$$

with the evolution operator $\tilde{U}(t)$, expressed in a chronologically ordered format, $t > t_1 > t_2 > \dots > t_n$:

$$\begin{aligned} \tilde{U}(t) &= \mathbb{1} + \sum_{n=1}^{\infty} \tilde{U}_n(t) \\ &= \mathbb{1} + \sum_{n=1}^{\infty} \int_{t_i}^t dt_1 \int_{t_i}^{t_1} dt_2 \cdots \int_{t_i}^{t_{n-1}} dt_n \tilde{L}(t_1) \\ &\quad \times \tilde{L}(t_2) \cdots \tilde{L}(t_n), \end{aligned} \quad (14)$$

where the $\tilde{U}_n(t)$ terms are defined by inspection. Since generally $[\tilde{L}(t), \tilde{L}(t')] \neq 0$ (for $t \neq t'$) the chosen evaluation order of the operators in the integral matters. Formally, with $\sigma(t_i)$ a constant matrix, the average of Eq. (13) is calculated to

$$\langle \sigma(t) \rangle = \langle \tilde{U}(t) \sigma(t_i) \rangle = \langle \tilde{U}(t) \rangle \sigma(t_i), \quad (15)$$

with the averaged evolution operator, $\langle \tilde{U}(t) \rangle = \mathbb{1} + \sum_{n=1}^{\infty} U_n(t)$, as

$$U_n(t) = \int_{t_i}^t dt_1 \int_{t_i}^{t_1} dt_2 \cdots \int_{t_i}^{t_{n-1}} dt_n M_n(t_1, t_2, \dots, t_n), \quad (16)$$

and $M_n(t_1, t_2, \dots, t_n)$ as in Eq. (B1) where $x(t)$ is replaced by $\tilde{L}(t)$, thus establishing the dependence on all field multitime moments (field’s coherences). In this form the $\langle \tilde{U}(t) \rangle$ operator as perturbative expansion may become impractical. In order to see this let’s assume the various terms in the expansion at a particular time—say “ t ”—and set the peak value of $\tilde{L}(t)$ as $L_0 \sim \mathcal{D}\mathcal{E}_0, \gamma_g \mathcal{I}_0, \gamma_a \mathcal{I}_0, \Gamma_a$. The first term grows with time as $\sim t L_0$, the second term as $\sim t^2 L_0^2$ and more generally a typical multitime term grows as $\sim (t L_0)^n$. For a well-behaved perturbative expansion we should require that $t L_0 \ll 1$. Therefore, regardless the peak strength ($\sim L_0$) the value of an arbitrary term will depend crucially on the field’s total duration, say τ_p through the combined parameter $\tau_p L_0 \sim \tau_p L_0 \ll 1$. Taking into account a modest value $L_0 \sim 1$ a.u. the evolution operator of Eq. (15) is invalidated as a legitimate perturbative expansion at longer times $t \gg 1$ a.u. (> 0.024 fs) than typical pulse durations of available FEL sources.

Based on the above observation, we aim to a perturbative expansion valid to arbitrarily long times via an expansion on cumulant averages instead on moment averages [40] (also, see Appendix B). Thus, we consider the series expansion the natural logarithm of $\langle \tilde{U}(t) \rangle$ in terms of the cumulant averages for the $\tilde{L}(t)$ operator:

$$\begin{aligned} K(t) &= \ln \langle \tilde{U}(t) \rangle = \sum_{n=1}^{\infty} \kappa_n(t), \\ \kappa_n(t) &= \int_{t_i}^t dt_1 \int_{t_i}^{t_1} dt_2 \cdots \int_{t_i}^{t_{n-1}} dt_n C_n(t_1, t_2, \dots, t_n), \end{aligned} \quad (17)$$

where $C_n(t_1, t_2, \dots, t_n)$ is the n^{th} cumulant as described in Appendix B. In the above expression a special prescription of the moments arises which leads to the so-called partially ordered cumulants [25,40]. For our special choice, which leads to $\langle \tilde{L}(t) \rangle = 0$, the lowest four cumulants are given by Eq. (B3). The higher-order cumulant expressions, in terms of the moments $M_n(t_1, t_2, \dots, t)$, can be found in the literature [25,40]. Again, it is important to note here that due to the noncommutative property of $\tilde{L}(t)$ it is essential to keep

track of the correct time ordering for the partially ordered cumulants.

With the above definitions the average of Eq. (13), using Eq. (17), can be written as

$$\langle \sigma(t) \rangle = \langle \tilde{U}(t) \sigma(t_i) \rangle = e^{K(t)} \sigma(t_i), \quad (18)$$

and by taking the time derivative of its right-hand side we obtain

$$\frac{d}{dt} (e^{K(t)} \sigma(t_i)) = \hat{T} [\dot{K}(t) e^{K(t)}] \sigma(t_i) = \dot{K}(t) \langle \sigma(t) \rangle, \quad (19)$$

where we used Eq. (18) to replace $\sigma(t_i)$ and thus to revert back to $\langle \sigma(t) \rangle$. In the above equation, the chronological operator \hat{T} ensures the proper time ordering ($t > t_1 > t_2 > \dots > t_n > t_i$). $\sigma(t_i)$ was moved outside the \hat{T} bracket since it is placed at the rightmost part of the equation in accordance with the assumed time ordering. $\dot{K}(t)$ is calculated by the use of Eq. (17), to eventually arrive at the desired EOM for the mean ensemble average of the density matrix elements:

$$\frac{d}{dt} \langle \sigma(t) \rangle = \sum_{n=1}^{\infty} \dot{\kappa}_n(t) \langle \sigma(t) \rangle, \quad (20)$$

with the time derivatives of $\kappa_n(t)$ expressed in terms of the multitime cumulants by

$$\begin{aligned} \dot{\kappa}_1(t) &= C_1(t), \\ \dot{\kappa}_n(t) &= \int_{t_i}^t dt_1 \int_{t_i}^{t_1} dt_2 \dots \int_{t_i}^{t_{n-2}} dt_{n-1} C_n(t, t_1, \dots, t_{n-1}), \end{aligned} \quad (21)$$

with $t_0 = t$. The explicit calculation of the cumulant coefficients, $\dot{\kappa}_n(t)$ up to $n = 4$ is given in the Appendix in Eqs. (C3)–(C5) and (C8).

The derivation of this formally exact expression did not necessitate any decorrelation approximation between the field's and $\sigma(t)$ fluctuations, nor any other particular statistical property such as stationarity or Gaussian-type multitime correlations. Equation (20) holds for general random fields and may be used as a perturbative expansion as long as the AC time τ_c is shorter than the other characteristic evolution times, a point which is discussed now. To show the argument, let's take the second term of the cumulant expansion $\dot{\kappa}_2(t)$:

$$\dot{\kappa}_2(t) = \int_{t_i}^t dt_1 \langle \tilde{L}(t) \tilde{L}(t_1) \rangle. \quad (22)$$

It is shown later that this term is proportional to $\sim \langle \mathcal{E}(t) \mathcal{E}^*(t_1) \rangle$ and $\sim \langle \mathcal{I}(t) \mathcal{I}(t_1) \rangle - \langle \mathcal{I}(t) \rangle \langle \mathcal{I}(t_1) \rangle$. For values of t and t_1 such that $|t - t_1| \gg \tau_c$ approximately $\langle \mathcal{E}(t) \mathcal{E}^*(t_1) \rangle \sim \langle \mathcal{E}(t) \rangle \langle \mathcal{E}^*(t_1) \rangle \sim 0$ and $\langle \mathcal{I}(t) \mathcal{I}(t_1) \rangle \sim \langle \mathcal{I}(t) \rangle \langle \mathcal{I}(t_1) \rangle$. In this case the integrand of $\dot{\kappa}_2(t)$ is short lived and approaches negligible values so that effectively the integral is restricted in the time interval $t - t_1 \sim \tau_c$. Therefore it is concluded that $\dot{\kappa}_2(t) \sim \Gamma_a \tau_c, \gamma_g^2 \mathcal{I}_0^2 \tau_c, \gamma_a^2 \mathcal{I}_0^2 \tau_c$ regardless of the evaluation of time t . This is in contrast to the evolution operator based on a moment expansion, Eq. (15), since the intensity term would still be contributing to the respective integral as $\sim t \gamma_g^2 \mathcal{I}_0^2, t \gamma_a^2 \mathcal{I}_0^2$. Analogous conclusions are reached for the higher cumulant terms which lead us to the necessary conditions for a converged perturbative expansion:

$$\gamma_i \mathcal{I}_0 \tau_c < 1, \quad i = g, a, \quad \text{and} \quad \Gamma_a \tau_c < 1, \quad (23)$$

with I_0 the maximum peak intensity. Thus we have concluded that the convergence conditions of the averaged EOMs is that the field intensity should not reach ionization saturation conditions within the time scale of the AC time.

A final point here is that our special choice of Eq. (5), which leads automatically to $\langle \tilde{L}(t) \rangle = 0$, makes the two perturbative expansions for the averaged EOMs (in moments and in cumulant averages), equivalent up to the second order; this is no longer the case, though, as we proceed to higher orders.

C. First two nonvanishing terms

Below we proceed by calculating the first two lowest orders of the cumulant expansion, $\dot{\kappa}_1(t)$ and $\dot{\kappa}_2(t)$. For the $\dot{\kappa}_1(t)$ term, by use of Eqs. (B3), (6)–(8), and (11) and by recalling $\langle \mathcal{E}(t) \rangle = \langle \tilde{\mathcal{I}}(t) \rangle = 0$, we find $\dot{\kappa}_1(t) = 0$. Using the same equations the $\dot{\kappa}_2(t)$ term of Eq. (22) is analyzed as

$$\begin{aligned} \dot{\kappa}_2(t) &= \bar{U}_b(t) \int_0^\infty d\tau_1 \langle \tilde{L}_b(t) e^{\int_{t-\tau_1}^t d\tau_1 \bar{L}_b(t, \tau_1)} \tilde{L}_b(t - \tau_1) \rangle \\ &\quad \times e^{-\int_{t-\tau_1}^t d\tau_1 \bar{L}_b(t, \tau_1)} \bar{U}_b^\dagger(t). \end{aligned} \quad (24)$$

To arrive at the last line in Eqs. (8) and (11) the initial time was set $t_i = -\infty$, followed by a change to the relative time variable $\tau_1 = t - t_1$. The last change has effectively removed the dependence of the equation on the initial time, as desired; as discussed a meaningful average law should lose any memory at times much longer than the fluctuation's correlation time. Keeping on with the evaluation, we take advantage of the shortness of the correlation time relative to the average intensity's slow variation and express the integral over the $\bar{L}_b(t, \tau_1)$ more conveniently:

$$\int_{t'}^t d\tau' \bar{L}_b(\tau') = L_0(t - t') + L_2 \langle W(t, t') \rangle, \quad (25)$$

where $\langle W(t, t') \rangle$ is the mean energy contained in the time interval $[t', t]$:

$$\langle W(t, t') \rangle = \int_{t'}^t d\tau' \langle \mathcal{I}(\tau') \rangle. \quad (26)$$

This term depends on the static part of the Hamiltonian and on the field's mean energy. A change of variables to $\tau_1 = t - t' > 0$ gives

$$\begin{aligned} \int_{t-\tau_1}^t d\tau_1 \bar{L}_b(t, \tau_1) &= L_0 \tau_1 + L_2 \int_{t-\tau_1}^t dt'' \langle \mathcal{I}(t'') \rangle \\ &\simeq (L_0 + L_2 \langle \mathcal{I}(t) \rangle) \tau_1 = \bar{L}_b(t) \tau_1. \end{aligned}$$

The approximate replacement in the second line is related to the slow variation of the field envelope. More specifically, since the field's AC functions decay with a rate $\sim 1/\tau_c$ practically the integral in Eq. (24), takes its main contributions for times τ_1 in the interval $[t - \tau_c, t]$; therefore the slowly varying $\mathcal{I}(t)$ is practically constant in this time interval. In quantitative

terms a Taylor expansion of $\langle I(t'' = t - \tau) \rangle$ gives

$$\int_{t-\tau_1}^t dt'' \langle \mathcal{I}(t'') \rangle = \int_0^{\tau_1} d\tau (\langle \mathcal{I}(t) \rangle \tau - \tau \langle \dot{\mathcal{I}}(t) \rangle + \dots) \\ \simeq \langle \mathcal{I}(t) \rangle \tau_1 - O(\tau_c \langle \dot{\mathcal{I}}(t) \rangle) \tau_1 / 2,$$

with the leading error term replaced by $\tau_1 \langle \dot{\mathcal{I}}(t) \rangle \simeq \tau_c \langle \dot{\mathcal{I}}(t) \rangle \ll 1$.

With the above in mind, now we transform back to the original EOMs $\sigma(t)$ using Eq. (8) to arrive at

$$\langle \dot{\sigma}_b(t) \rangle = \left[\bar{L}_b(t) + \int_0^\infty d\tau_1 \mathcal{K}_2(t, t - \tau_1) \right] \langle \sigma_b(t) \rangle, \quad (27)$$

with the extra term $\mathcal{K}_2(t, t_i)$ clearly generated from the averaging process. The term inside the integrand is nonvanishing

for times of the order of the field's correlation time τ_c , since it depends on the first two AC functions. More specifically, direct substitution of Eqs. (6) and (7) gives

$$\mathcal{K}_2(t, t - \tau_1) = L_1 e^{\bar{L}_b(t)\tau_1} L_1^T e^{-\bar{L}_b(t)\tau_1} \langle \mathcal{E}(t) \mathcal{E}^*(t - \tau_1) \rangle \\ + L_1^T e^{\bar{L}_b(t)\tau_1} L_1 e^{-\bar{L}_b(t)\tau_1} \langle \mathcal{E}^*(t) \mathcal{E}(t - \tau_1) \rangle \\ + L_2^2 \langle \mathcal{I}(t) \mathcal{I}(t - \tau_1) \rangle. \quad (28)$$

Explicit substitution in Eqs. (28) and (27) of L_i $i = 0, 1, 2$ [Eqs. (A9)–(A11)] leads to our main expressions for the averaged EOMs of the bound states:

$$\frac{d}{dt} \langle \sigma_{gg}(t) \rangle = -[\gamma_g \langle \mathcal{I}(t) \rangle - \gamma_g^2 S_{2t}(0) + 2\text{Re}\{\mathcal{D}^2 S_{1t}(\delta_+)\}] \langle \sigma_{gg}(t) \rangle + 2|\mathcal{D}|^2 \text{Re}\{S_{1t}(\delta_-)\} \langle \sigma_{aa}(t) \rangle, \quad (29a)$$

$$\frac{d}{dt} \langle \sigma_{aa}(t) \rangle = -[\Gamma_a + \gamma_a \langle \mathcal{I}(t) \rangle - \gamma_a^2 S_{2t}(0) + 2\text{Re}\{\mathcal{D}^* S_{1t}(\delta_-)\}] \langle \sigma_{aa}(t) \rangle + 2|\mathcal{D}|^2 \text{Re}\{S_{1t}(\delta_+)\} \langle \sigma_{gg}(t) \rangle, \quad (29b)$$

$$\frac{d}{dt} \langle \sigma_{ag}(t) \rangle = -[\delta + \Delta \langle \mathcal{I}(t) \rangle - \Delta^2 S_{2t}(0) + \{\mathcal{D}^2 S_{1t}(-\delta_+) + \mathcal{D}^{*2} S_{1t}(-\delta_-)\}] \langle \sigma_{ag}(t) \rangle, \quad (29c)$$

where the averaged dynamic detunings, $\delta_\pm \equiv \delta_\pm(t)$, are defined by

$$\delta_\pm(t) = t[\delta_0 + (s_a - s_g) \langle \mathcal{I}(t) \rangle] \pm \frac{\Gamma_a + (\gamma_a - \gamma_g) \langle \mathcal{I}(t) \rangle}{2}. \quad (30)$$

The coefficients in Eq. (29) are expressed as the Laplace transforms of the AC functions of the field and the intensity, respectively:

$$S_{1t}(\delta) = \int_0^\infty d\tau \langle \mathcal{E}(t) \mathcal{E}^*(t - \tau) \rangle e^{-\delta\tau}, \quad (31)$$

$$S_{2t}(0) = \int_0^\infty d\tau (\langle \mathcal{I}(t) \mathcal{I}(t - \tau) \rangle - \langle \mathcal{I}(t) \rangle \langle \mathcal{I}(t - \tau) \rangle). \quad (32)$$

The complex quantity $S_{1t}(\delta)$ is closely related to a time-dependent frequency spectrum and for such long pulses, where stationarity conditions of the field's statistical properties are reached, approach the field's power spectrum via the Wiener-Khinchin theorem [17]. Under the later (stationarity) assumption it can also be shown that the $S_{2t}(0)$ is proportional to the field's average energy standard deviation, $\langle \Delta W^2(t) \rangle$. Equation (29) is the result of the lowest-order nonvanishing approximation of an infinite term expansion and have general applicability with respect to the field's fluctuations on the proviso of the conditions set by Eq. (23); as such there is an associated upper limit in the intensity for the condition to be fulfilled.

Explicit, analytical, expressions for the S_{1t} , S_{2t} are given later in the text for the case where the field is considered non-stationary, Gaussian, and square-exponentially time correlated coherence functions.

D. Equations for the continuum populations

Now we turn to the derivation of the averaged populations of the continuum part of the density matrix, namely, the time evolution law for $\langle \sigma_{cc}(t) \rangle$ and $\langle \sigma_{c'c'}(t) \rangle$. These equations constitute an inhomogeneous set of stochastic equations dependent on the statistically correlated terms, $\mathcal{I}(t)$, $\sigma_{gg}(t)$, and $\sigma_{aa}(t)$:

$$\dot{\sigma}_{cc} = -\gamma_c \mathcal{I}(t) \sigma_{cc} - \dot{\sigma}_{gg} - \dot{\sigma}_{aa}, \quad (33a)$$

$$\dot{\sigma}_{c'c'} = \gamma_a \mathcal{I}(t) \sigma_{c'c'}. \quad (33b)$$

The statistics of $\mathcal{I}(t)$ is given from the outset whereas this is not the case for the random populations, $\sigma_{gg}(t)$, $\sigma_{aa}(t)$; their statistical properties are determined by the atomic system's response. Various methods are available to derive the averaging form of the above equations but since here we focus on the first nonvanishing terms for arbitrary stochastic fields we may repeat the method applied in the bound part of the density matrix. For this, the first task is to bring the continuum equations in the form of Eq. (5). We achieve this by augmenting the set of the continuum equations to include the $\dot{\sigma}_{gg}$, $\dot{\sigma}_{aa}$ and define $\sigma_c(t) = (\sigma_{cc}(t), \sigma_{c'c'}(t), 1)$ with $p_b(t) = \sigma_{gg}(t) + \sigma_{aa}(t)$. Now we can write

$$\dot{\sigma}_c(t) = [\bar{L}_c(t) + \tilde{L}_c(t)] \sigma_c(t), \quad (34)$$

with $\sigma_c(t_i) \equiv (0, 0, 1)$. The mean average and the random parts, $\bar{L}(t)$, $\tilde{L}(t)$, are given by

$$\bar{L}_c(t) = \begin{pmatrix} -\gamma_c \langle \mathcal{I}(t) \rangle & 0 & 0 \\ 0 & \gamma_a \langle \mathcal{I}(t) \rangle & 0 \\ 0 & 0 & 0 \end{pmatrix}, \quad (35)$$

$$\tilde{L}_c(t) = \begin{pmatrix} -\gamma_c \tilde{\mathcal{I}}(t) & 0 & \dot{p}_b(t) \\ 0 & \gamma_a \tilde{\mathcal{I}}(t) & 0 \\ 0 & 0 & 0 \end{pmatrix}. \quad (36)$$

Repeating the steps described in the previous sections and keeping only the first two terms of the perturbative expansion we arrive at an equation analogous to Eq. (27). The end result for the averaged populations is

$$\begin{aligned} \langle \dot{\sigma}_{cc}(t) \rangle &= -\gamma_c \langle \mathcal{I}(t) \rangle \langle \sigma_{cc} \rangle - \langle \dot{\sigma}_{gg} \rangle - \langle \dot{\sigma}_{aa} \rangle \\ &\quad + \gamma_c S_{2t}(0) [\gamma_c \langle \sigma_{cc} \rangle - \gamma_g \langle \sigma_{gg} \rangle - \gamma_a \langle \sigma_{aa} \rangle], \end{aligned} \quad (37a)$$

$$\langle \dot{\sigma}_{c'c'}(t) \rangle = +[\gamma_a \tilde{\mathcal{I}}(t) + \gamma_a^2 S_{2t}(0)] \langle \sigma_{aa} \rangle. \quad (37b)$$

III. THE CASE OF A GAUSSIAN RANDOM FIELD

Having established the approximate averaged equations we now proceed to further specialization for the important case of pulsed fields obeying Gaussian statistics. The field is assumed with an envelope of the form,

$$\mathcal{E}_0(t) = \mathcal{E}_0 e^{-\chi t^2/2\tau_p^2}, \quad (38)$$

with the χ complex, for pulses modeling FEL radiation [17,19]. This choice specifies the statistically averaged intensity via Eq. (1) as

$$\langle \mathcal{I}(t) \rangle = \langle |\mathcal{E}(t)|^2 \rangle = \mathcal{E}_0^2 e^{-t^2/\tau_p^2}. \quad (39)$$

Note that the FWHM duration of the mean intensity is related to τ_p by $\tau_{\text{FWHM}} = \tau_p \sqrt{4 \ln 2}$. The reader should not be confused and associate fields with this particular choice of a Gaussian envelope with fields obeying Gaussian statistics; it is unrelated to the Gaussian statistical properties of the field and the square-exponential decay form of the AC functions. We could have chosen any other analytical form for the envelope of the mean intensity to model the actual pulse.

In view of Eq. (1), the field's fluctuations are modeled through the stationary random field $\epsilon(t)$, obeying complex Gaussian ensemble statistics [21],

$$\langle \epsilon(t) \rangle = \langle \epsilon(t)\epsilon(t') \rangle = \langle \epsilon^*(t)\epsilon^*(t') \rangle = 0. \quad (40)$$

The latter property gives for the nonstationary first-order field coherence,

$$\langle \mathcal{E}(t)\mathcal{E}^*(t') \rangle = \mathcal{E}_0(t)\mathcal{E}_0^*(t') \langle \epsilon(t)\epsilon^*(t') \rangle. \quad (41)$$

Under these conditions the first-order coherence function of the intensity can be related to the first-order coherence of the field:

$$\langle \mathcal{I}(t)\mathcal{I}(t') \rangle = \langle \mathcal{I}(t) \rangle \langle \mathcal{I}(t') \rangle + |\langle \mathcal{E}(t)\mathcal{E}^*(t') \rangle|^2. \quad (42)$$

This gives for the random part of the intensity,

$$\langle \tilde{\mathcal{I}}(t)\tilde{\mathcal{I}}(t') \rangle = |\langle \mathcal{E}(t)\mathcal{E}^*(t') \rangle|^2, \quad (43)$$

which effectively leads to expressing $S_{1t}(\pm\delta_{\pm})$ and $S_{2t}(0)$ exclusively in terms of the first-order field's coherence function $\langle \mathcal{E}(t)\mathcal{E}^*(t') \rangle$.

a. Square-exponentially correlated first-order coherence. This consists of assuming the dependence below:

$$\langle \epsilon(t)\epsilon^*(t') \rangle = e^{-(t-t')^2/2\tau_c^2}. \quad (44)$$

Regarded as a sufficiently good approximation to actual FEL fields, this model has been studied in detail from the viewpoint of a shot-noise random field resulting in a random intensity with exponential probability distribution law and fluctuating

energy $W(t, t_i)$ of Gamma distribution [17,18,20]. The required integrations are performed analytically to provide the closed-form expressions,

$$S_{1t}(\delta) = \tau_{\text{coh}} \sqrt{\pi} \langle \mathcal{I}(t) \rangle \lambda w \left(\lambda \left(\frac{\chi^* t}{M\tau_p} - \delta\tau_{\text{coh}} \right) \right), \quad (45a)$$

$$S_{2t}(0) = \tau_{\text{coh}} \sqrt{\pi} \frac{\langle \mathcal{I}(t) \rangle^2}{2} w \left(\frac{t}{M\tau_p} \right), \quad (45b)$$

$$M = \frac{\tau_p}{\tau_{\text{coh}}}, \quad \tau_{\text{coh}} = \frac{\tau_p \tau_c}{\sqrt{\tau_p^2 + \tau_c^2}}, \quad (45c)$$

$$\chi = 1 - ik, \quad \lambda = \frac{1}{\sqrt{2(1 + ik/M^2)}}, \quad (45d)$$

where $w(z) = e^{z^2} (1 + \text{erf}(z))$, $\text{erf}(z)$ being the error function, and $k = 1/\sqrt{3}$ for FEL pulses. These expressions are very closely related to the Voigt profile functions, originating from the convolution of Gaussian and Lorentzian spectra. The Gaussian character of the resulting spectrum is exclusively due to the field's properties, namely the envelope's mean-value time dependence ($\sim \tau_p$) and coherence time ($\sim \tau_c$). On the other hand the Lorentzian character is due to near-resonance effects and thus includes information about the atomic system and its response to the atomic field via the mean-average detunings $\delta_{\pm}(t)$; as the latter quantity includes information only about the mean intensity $\langle \mathcal{I}(t) \rangle$ it may be inferred that the Lorentzian character of the lineshape is not influenced by the field's fluctuations. The M parameter is a measure of the number of random "spikes" during the pulse and of the strength of the fluctuations as its inverse approximates $\langle (\Delta W)^2 \rangle / \langle W \rangle^2$ where $\langle (\Delta W)^2 \rangle$ is the standard deviation of $W(t)$. Finally the τ_{coh} is known as the field's *coherence time* and may be alternatively defined via the normalized field's coherence function. More detail on this and the various field parameters can be found in Ref. [17].

For longer pulses ($M \gg 1$ ($\tau_p \gg \tau_c$)), S_{1t}, S_{2t} take a simpler form; at times $t \sim M\tau_p$ the mean intensity $\langle \mathcal{I}(t) \rangle$ is negligible (decays as $e^{-2(t/\tau_p)^2}$) and we may consider the earlier times $t \sim \tau_p$ where the approximation $w(t/M\tau_p + b) \sim w(0 + b)$ can be adopted. For such pulses the time dependence and the frequency dependence in $S_{1t}(\delta)$ factorize as below:

$$S_{1t}(\delta) \simeq \tau_{\text{coh}} \sqrt{\pi} \frac{\langle \mathcal{I}(t) \rangle}{\sqrt{2}} w \left(\frac{-\delta\tau_{\text{coh}}}{\sqrt{2}} \right), \quad (46a)$$

$$S_{2t}(0) \simeq \tau_{\text{coh}} \sqrt{\pi} \frac{\langle \mathcal{I}(t) \rangle^2}{2}. \quad (46b)$$

From Eq. (46a) it is easier to clarify the role of various parameters in the lineshape profile; we see that in the argument of Eq. (46a) the smooth time dependence on the mean intensity is still present as seen from Eq. (30). So S_{1t} depends on the atomic parameters and the smooth mean intensity envelope and the field's coherence time τ_{coh} (note that for $M \gg 1$, $\tau_{\text{coh}} \rightarrow \tau_c$). It's not difficult to see that with decreasing τ_{coh} the lineshape takes a Lorentzian shape regardless of the field's intensity. In such conditions, the shape of the Lorentzian profile will not contain any direct influence of the field's fluctuation statistics; this will depend on the parameters included in the δ_{\pm} mean detunings. In Fig. 2 we provide the

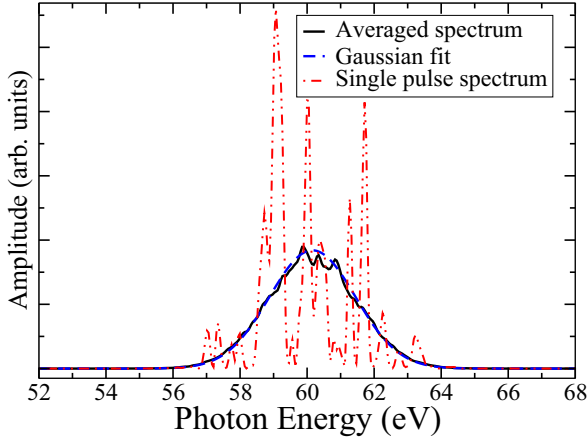


FIG. 2. Frequency spectrum for a pulse with central frequency $\omega = 60.154$ eV, coherence time $\tau_c = 0.5$ fs, and total pulse duration $\tau_p = 7$ fs. The M parameter is equal to 14. Solid black line represents the averaged spectrum, dashed blue line is its Gaussian fit with width ~ 1.32 eV while dot-dashed red line is the spectrum corresponding to one of the pulse's realizations.

ensemble-averaged frequency spectrum obtained for a pulse with $\tau_c = 0.5$ fs and $\tau_p = 7$ fs. Having included circa 300 pulses in the ensemble we see that the averaged profile tends to a Gaussian shape as expected. Fitting with a Gaussian envelope we find that the pulse's frequency bandwidth is circa 1.32 eV.

b. Exponentially correlated first-order coherence. Now we assume the AC coherence function to exhibit exponential correlation behavior of the type,

$$\langle \epsilon(t)\epsilon^*(t') \rangle = e^{-|t-t'|/2\tau_c}. \quad (47)$$

In Eq. (38) we take $\chi = 1$ and obtain for S_{1t} and S_{2t} ,

$$S_{1t}(\delta) = \tau_p \sqrt{\pi} \frac{\langle \mathcal{I}(t) \rangle}{\sqrt{2}} w\left(\frac{\tau_\delta}{\sqrt{2}}\right), \quad (48)$$

$$S_{2t}(0) = \tau_p \sqrt{\pi} \frac{\langle \mathcal{I}(t) \rangle^2}{2} w(\tau_0), \quad (49)$$

$$\tau_\delta = \frac{t}{\tau_p} - \left(\frac{1}{2\tau_c} + \delta \right) \tau_p, \quad (50)$$

thus still showing a Voigt profile shape. Using the asymptotic value $w(z \gg 1) \rightarrow 1/z\sqrt{\pi}$, we find the corresponding approximate expressions for longer pulses ($\tau_p \gg \tau_c$),

$$S_{1t}(\delta) = \langle \mathcal{I}(t) \rangle \frac{2\tau_c}{1 + 2\delta\tau_c}, \quad (51)$$

$$S_{2t}(0) = \langle \mathcal{I}(t) \rangle^2 \tau_c, \quad (52)$$

show clearly a Lorentzian-like shape.

IV. RESULTS AND DISCUSSION

In this section we apply the averaged equations for the resonance ionization of helium via the $2s2p^1P$ AIS located circa 60.154 eV above its ground state. First, we compare the yields obtained from the averaged equations with those obtained from a MC set of calculations in order to establish numerically

TABLE I. Atomic parameters in a.u. used for the He($2s2p$) AIS resonance. The values for the effective matrix element d_{ga} is calculated by $4|d_{ga}|^2 = q_a^2 \Gamma_\alpha \gamma_g$.

Parameters	Values (a.u.)
(E_a, q_a)	(2.211, -2.733)
d_{ga}	0.0358
Γ_α	0.00137
γ_g	0.494
γ_c	0.426

the range of validity of the approximation. Then we examine the role of the field's—and the intensity's—coherence functions on the ionization process. Finally, we proceed to compare the effects the field's correlation time dependence on the AIS lineshape. The specific set of the atomic parameters in the following calculations are given in Table I. These values have been calculated some time earlier with a well-established atomic calculation package [31,41,42].

A. Comparison with the Monte Carlo calculations

Using the averaging method, not only the computational demands are significantly reduced but a clearer insight of the ionization dynamics under stochastic fields may be obtained. To investigate the validity of the equations we compare the results obtained with the averaged equations against those obtained via a Monte Carlo (MC) approach. In the latter method the original set of the DM equations [Eq. (3)] is solved for a large number of (random) realizations of the field. At the end, the results are collected and are accordingly averaged. In principle, when the number of the MC trials goes to infinity (in practice this number depends on the problem) one should expect the results between the two calculational methods (MC and averaged equations) to coincide to a high degree.

In Fig. 3, we plot the ionization yields, obtained from the MC simulation and the averaged equations [Eqs. (29) and (37)], for different peak intensities of the pulse. The irregular behavior of the MC yield is the result of the inherent randomness present in the FEL field, which diminishes with the total number of MC trials increasing. As the computational time increases, we chose 300 simulations to calculate the MC average, as the tendency is clearly evident. For the following calculations, we set $\tau_p = 7$ fs, $\tau_c = 0.5$ fs, and $M = 14$.

The plots (a)–(c) of Fig. 3 show the single ionization yield without including the subsequent ionization step from He⁺ and without considering ionization directly from the AIS state. For this, we have assumed $\gamma_c = \gamma_a = 0$ and calculated for three different peak intensities, 10^{13} W/cm², 10^{14} W/cm², and 10^{15} W/cm². Simple inspection of the plots shows that for the higher intensity the agreement between the two methods is less satisfactory, especially in the proximity of the resonance. First, its modified shape indicates that the field is already so strong that on average the atom oscillates between the states $|g\rangle$ and $|a\rangle$ (Rabi oscillation) before it eventually “escapes” irreversibly to the continua $|c\rangle$ and $|c'\rangle$. These nonlinear transitions lead inevitably to a modified ionization profile. For this highest peak intensity the perturbative terms due to the intensity correlation take the peak values $\gamma_g \mathcal{I}_0 \tau_c \sim 0.3$ ($\Gamma_\alpha \tau_c \sim 0.028$) in fair consistency with the conditions of Eq. (23).

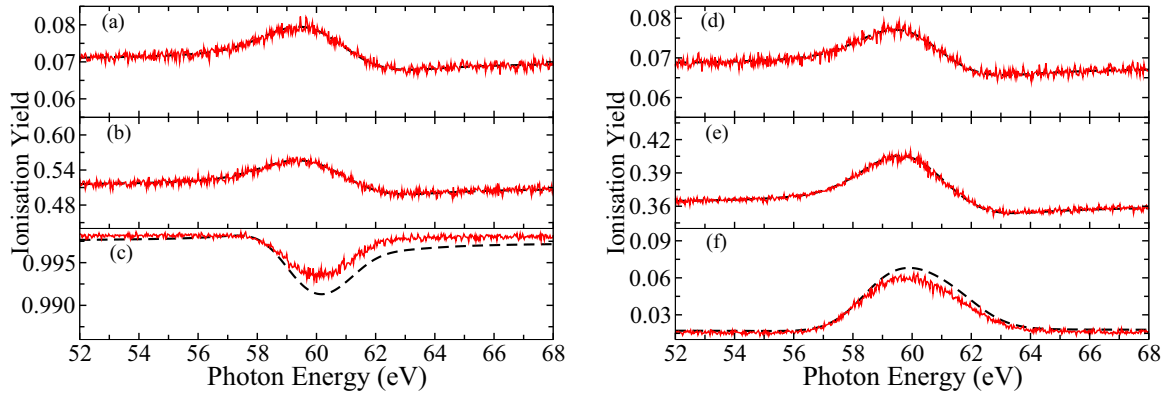


FIG. 3. Comparison of ionization yields obtained from the Monte Carlo method (red solid curve) and averaged density matrix equations (black dashed curve) for peak intensities of 10^{13} W/cm 2 , 10^{14} W/cm 2 , and 10^{15} W/cm 2 (top to bottom, respectively). $\gamma_c = 0$ a.u. for (a)–(c) and $\gamma_c = 0.426$ a.u. for (d)–(f). Other parameters are $\tau_p = 7$ fs, $\tau_c = 0.5$ fs ($M = 14$).

The cumulant perturbative expansion was truncated in the second order which includes the first two coherence functions of the field. So, at this peak intensity the next perturbative term should be included in the averaged equations, but for the intensities currently available at this wavelength and the current purposes of this work it's not vital to include the next term of the expansion; however, we'll be returning to this matter later in the conclusion section.

In an actual experiment, further ionization of the singly ionized He takes place and a proper treatment requires one to take into account the complete set of the density matrix equations. The plots (d)–(f) on the right side of the Fig. 3 include the ionization channel from He $^+$ to He $^{+2}$ ($\gamma_c = 0.436$ a.u. but $\gamma_a = 0$). The first thing to note is the broadened yield around resonance. In contrast, a deterministic (and Fourier-limited) pulse would have developed a sharp asymmetric peak near the resonance energy of $2s2p$, i.e., 60.154 eV (2.211 a.u.), typical of an AIS resonance with the $q = -2.733$ Fano parameter. The width of this resonance would reflect the AIS width Γ_a . Here, the fluctuations of the FEL field have smoothed this sharp resonance resulting to a broadened shape.

On another note, in the same figure we can see that for lower peak intensities the He $^+$ yields obtained for $\gamma_c = 0$ (left plots) are close to those when $\gamma_c = 0.426$ a.u. (right plots). Considering only the right side plots of Fig. 3, we notice an increase in the yield value from (d) to (e), which follows the trend of (a) to (b). But the same trend is lost in (f). This is due to the enhanced He $^+$ generated at times before the pulse reached its peak, followed by its quick ionization to He $^{+2}$. Obviously this is not the case for lower peak intensities where He $^+$ is generated past the pulse's peak. This is shown clearly at the bottom panel of Fig. 4 where as soon as the population of He $^+$ reaches a maximum, it decays rapidly into He $^{2+}$ for the highest peak intensity ($\sim 10^{15}$ W/cm 2); in contrast with what is observed at the upper panel of the same figure, where the He $^+$ populations develop past the pulse's peak value (assumed at $t = 0$).

It's instructive to see how it compares the averaged ionization profile with a single-shot ionization profile as well as how it compares with the profile obtained by convoluting the AIS's Fano profile with the ensemble-averaged frequency pulse's spectrum. The former case is shown in the upper plot

of Fig. 5 while the latter one in the lower plot of the same figure. The atomic and FEL radiation parameters are chosen as those of Fig. 3(a). As expected, the single-shot ionization yield profile is highly irregular, reflecting the random nature of the pulse's temporal profile. The convolution ionization profile was obtained as

$$Y(\omega) = \int_{-\infty}^{\infty} d\omega' \overline{\mathcal{I}(\omega')} F(\omega - \omega'), \quad (53)$$

where the AIS's Fano profile represented by $F(\omega) \sim [(q_a + \epsilon_\omega)/(1 + \epsilon_\omega^2) - 1]/(q_a^2 \Gamma_a)$ with $\epsilon_\omega = 2(E_g + \omega - E_a)/\Gamma_a$. With this definition, $F(\omega)$ has as a limiting case a Lorentzian shape for $q \rightarrow \infty$. $\overline{\mathcal{I}(\omega)} = \langle |\mathcal{E}(\omega')|^2 \rangle$ represents the obtained ensemble-averaged frequency profile. In the same figure [bottom panel of Fig. (5)] we show the corresponding MC calculations. The ensemble-averaged profile of the present method is in excellent agreement with the MC calculations while the convolution method leads to a more symmetric profile. It is worth noting here that the convolution profile has been multiplied such that to match the ionization profile produced from the full time-dependent MC and the averaged

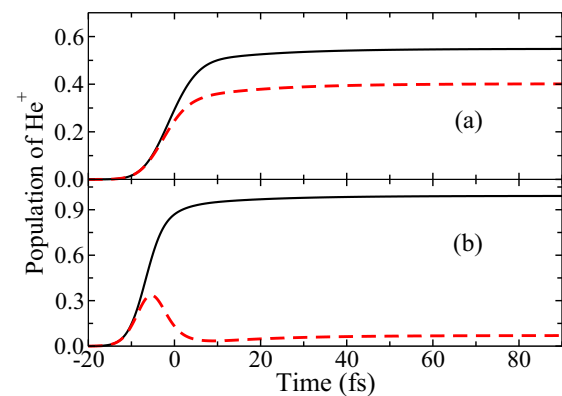


FIG. 4. Comparison of He $^+$ yield when its further ionization is taken into account (red dashed curves) and when it is not (black solid curves), for the peak intensities 10^{14} W/cm 2 (a) and 10^{15} W/cm 2 (b). The yields were obtained at the resonance frequency 60.154 eV and for $\tau_p = 7$ fs, $\tau_c = 0.5$ fs ($M = 14$).

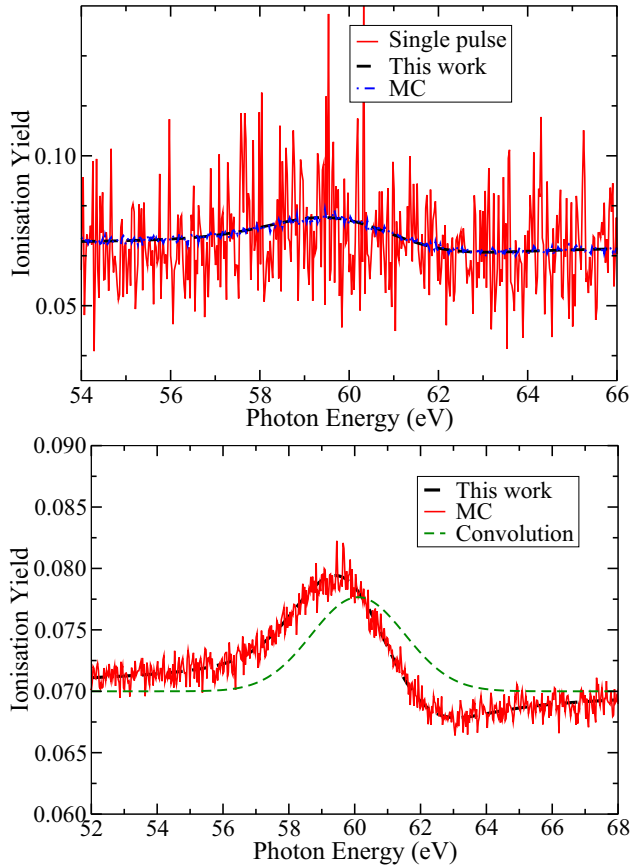


FIG. 5. (Upper panel) Single-ionization yield for one realization of the random pulse (red solid line), and its corresponding ensemble average (over 300 realizations) obtained from the averaged EOMs (black dashed line) and the MC method (blue dashed line). (Bottom panel) He^+ yields using the convolution of the AIS Fano shape with the averaged pulse profile (green dashed line), Eq. (53), the averaged EOMs (black line), and the MC approach (red line). The yields were obtained at the resonance frequency 60.154 eV and for $\tau_p = 7$ fs, $\tau_c = 0.5$, and peak intensity $10^{13} \text{W}/\text{cm}^2$.

EOM equations. For the particular helium AIS where $q_a = -2.733$ it is expected the convolution method to produce a peak rather than a dip in the resonance position [43,44]. Nevertheless the convolution method is of limited use as it implies a weak-field excitation where the ionization profile is not severely distorted due to Rabi oscillations between the ground and the AI state.

B. Effects of the field's AC shape

We now investigate the effects of the shape of a Lorentzian-dependent AC coherence function on the lineshape and compare with a square-exponential dependence.

It is easily shown that a stationary (or nearly stationary) field of an exponentially correlated coherence function has a Lorentzian-like power spectrum whereas for a square-exponential-dependent coherence function the spectrum is Gaussian. We want to see how the field's AC function affects the AIS lineshape; we compare the results for the two different AC shapes for the same coherence time τ_c , one exponentially

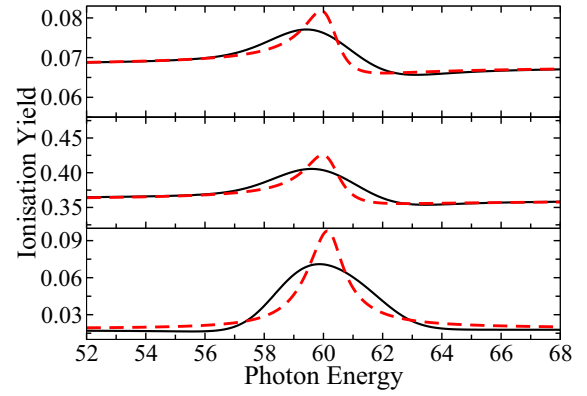


FIG. 6. Comparison of the ionization yields obtained by using Gauss correlation (black solid curve) and Lorentz correlation (red dashed curve) for the peak intensities of $10^{13} \text{W}/\text{cm}^2$, $10^{14} \text{W}/\text{cm}^2$, and $10^{15} \text{W}/\text{cm}^2$, respectively. Other parameters are $\tau_p = 7$ fs, $\tau_c = 0.5$ fs ($M = 14$).

correlated [see Eq. (47)] and the other approximately close to the one produced from FEL sources, especially for pulses of longer duration [17,20], being the square exponential of Eq. (44).

In Fig. 6 we plot the yields obtained for three different intensities, from top to bottom, the peak intensity increases as $10^{13} \text{W}/\text{cm}^2$, $10^{14} \text{W}/\text{cm}^2$, and $10^{15} \text{W}/\text{cm}^2$, respectively. We notice that the peaks have different values with the exponentially correlated fields developing a narrower shape, while their tails are very close each other. Therefore, there is a notable difference in the yields in the resonance region which can be attributed exclusively in the choice of the AC temporal dependence.

C. Effects of Field's correlation time on the AIS lineshape

As we have already established the accuracy of the averaging technique, we may now consider a larger pulse duration of $\tau_p = 45$ fs (corresponding to $\tau_{\text{FWHM}} \approx 75$ fs) (corresponding to FWHM laser bandwidth of 0.4 eV) and study the effects of different correlation times of the field on the AIS lineshape using the averaging method. This pulse is close to parameters used in Ref. [45].

In Fig. 7, the ionization yield obtained for various correlation times and peak intensity is $10^{13} \text{W}/\text{cm}^2$. It is seen that, as the correlation time decreases the yield value at the resonance's position drops and the AIS lineshape becomes broader. τ_c is directly related to the laser bandwidth and therefore, a decrease in the correlation time of the field implies an increase in the laser bandwidth which manifests as the broadening of the AIS lineshape, so the broadening effect is compensated by the drop of the resonance peak. As, at the tails of the yield, the values are quite constant it is concluded that the coherence time effects are manifested mainly around the resonance peak. This behavior is also consistent with the behavior of S_{I_t} in Eq. (46a) where towards smaller τ_c the line-shape gradually broadens at the wings following a Lorentzian-like trend.

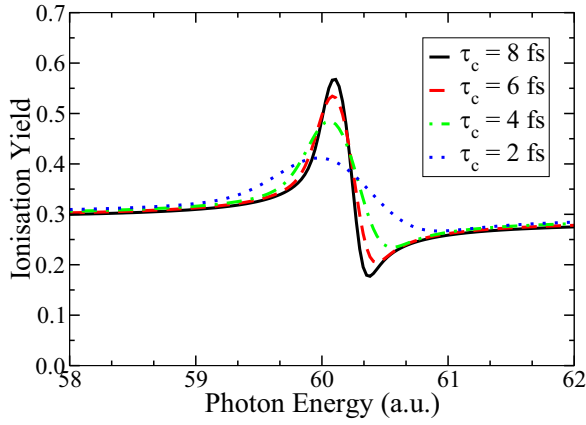


FIG. 7. Comparison of the ionization yield obtained by using Gaussian form of the field's autocorrelation function at 10^{13} W/cm² for different coherence times τ_c : 2 fs (black curve), 4 fs (red curve), 6 fs (green curve), and 8 fs (blue curve). At resonance, the yield is highest for the longest coherence time and it gradually decreases as the τ_c is decreased. The pulse duration used is $\tau_p = 45$ fs.

V. CONCLUSION

We presented a cumulants-based perturbative method to derive the averaged EOMs of the mean density matrix elements which describe the resonant ionization of atomic systems under stochastic fields. We have applied its second-order truncated expansion for the near-resonant ionization (via He $2s2p$ AIS state at ~ 60.154 eV) and compared with MC calculations. The convergence of the perturbation expansion depends on the field's strength and its coherence AC time; the basic assumption is that the coherence AC time is shorter than any other characteristic evolution time imposed by the field or the atomic structure itself (inverse Rabi-excitation amplitude and photoionization, autoionization width). We found that in general a Voight profile for the AIS is to be expected; this profile depends both on the field and the intensity AC functions.

There are a number of other statistical aspects of the atom-FEL radiation interactions which necessitate further study in order to identify more comprehensively the role of the fluctuations in the ionization process. First, possible improvements of the averaging procedure needs to be investigated; one such alternative is based on the atomic physics projection-operator method, but now applied to stochastic problems, also leading to averaged equations for the density matrix elements, known as the Nakajima-Zwanzig equation [46,47]; nevertheless this equation has a non-Markovian structure which implies knowledge of the average density matrix at all previous times is needed: $\langle \sigma(t') \rangle$, $t' < t$, and not only at one time, $\langle \sigma(t) \rangle$, as the Markov-type derived equation [Eq. (20)].

Along similar lines it is within our interests to improve the method and drop the assumption of τ_c as the shortest characteristic time. Another route we would like to focus on is to provide a method where higher-order terms of the perturbative expansion can be calculated more automatically and efficiently for arbitrary FEL fields without the need to invoke the Gaussian statistics requirement; this will allow one to model a larger class of problems than those that can be treated with the present method. Finally an alternative direction is to

deal with problems where the statistics of the system's density matrix itself (beyond its average) is required; this calls for two-time averages of the type $\langle \sigma(t)\sigma(t') \rangle$ to be calculated; the method presented in this work, can be also applied for such averages to be calculated, of course within the limitations of the short-correlation time τ_c .

ACKNOWLEDGMENTS

T.K. wants to acknowledge the support by the Education, Audiovisual and Culture Executive Agency (EACEA) EXTATIC-Erasmus Mundus Joint Doctorate Programme Project No. 2011 0033.

APPENDIX A: EVOLUTION MATRICES

If we define the near-resonant detuning δ_0 by

$$\delta_0 = E_a - E_g - \omega, \quad (\text{A1})$$

then the complex detunings Δ , δ are given as

$$\delta = i\delta_0 + \frac{\Gamma_a}{2}, \quad \Delta = i(s_a - s_g) + \frac{\gamma_g + \gamma_a}{2}, \quad (\text{A2})$$

with s_g, s_a the peak intensity ac-Stark shifts of the respective states. The interference matrix element is

$$\mathcal{D} = d_{ga} \left(1 - \frac{i}{q_a} \right) = |\mathcal{D}| e^{-i\phi_a}, \quad (\text{A3})$$

where d_{ga} is the real part of the transition matrix element between the ground $|g\rangle$ and the excited $|a\rangle$ state and q_a is the q-Fano parameter. We should emphasize (within the Fano ionization picture) the strict relation between the involved dynamics parameters:

$$4|d_{ga}|^2 = q_a^2 \Gamma_a \gamma_g, \quad (\text{A4})$$

$$\gamma_g = 2\pi |d_{gc}|^2, \quad \gamma_c = 2\pi |d_{c'c}|^2, \quad (\text{A5})$$

$$\gamma_a = 2\pi |d_{ac'}|^2, \quad \Gamma_a = 2\pi \left| \langle a | \frac{1}{r_{12}} | c \rangle \right|^2, \quad (\text{A6})$$

and

$$s_a = P \int d\epsilon_{c'} \frac{|d_{ac'}|^2}{\epsilon_a + \omega - \epsilon_{c'}}, \quad (\text{A7})$$

$$s_g = P \int d\epsilon_c \frac{|d_{gc}|^2}{\epsilon_g + \omega - \epsilon_c}, \quad (\text{A8})$$

with P denoting the principal value integral.

The constant matrices L_i , $i = 0 - 2$ are as below:

$$L_0 = - \begin{pmatrix} 0 & 0 & 0 & 0 \\ 0 & \Gamma_a & 0 & 0 \\ 0 & 0 & \delta & 0 \\ 0 & 0 & 0 & \delta^* \end{pmatrix}, \quad (\text{A9})$$

$$L_1 = i \begin{pmatrix} 0 & 0 & -\mathcal{D} & 0 \\ 0 & 0 & \mathcal{D}^* & 0 \\ 0 & 0 & 0 & 0 \\ \mathcal{D}^* & -\mathcal{D} & 0 & 0 \end{pmatrix}, \quad (\text{A10})$$

with L_1^T representing the transpose of L_1 . Finally,

$$L_2 = - \begin{pmatrix} \gamma_g & 0 & 0 & 0 \\ 0 & \gamma_a & 0 & 0 \\ 0 & 0 & \Delta & 0 \\ 0 & 0 & 0 & \Delta^* \end{pmatrix}. \quad (\text{A11})$$

With the above definitions $\tilde{L}_b(t)$ takes the following explicit form,

$$\tilde{L}_b(t) = \begin{pmatrix} -\gamma_g \tilde{\mathcal{I}}(t) & 0 & -i \tilde{\mathcal{E}}(t) \mathcal{D} & i \tilde{\mathcal{E}}^*(t) \mathcal{D}^* \\ 0 & -\gamma_a \tilde{\mathcal{I}}(t) & i \tilde{\mathcal{E}}(t) \mathcal{D}^* & -i \tilde{\mathcal{E}}^*(t) \mathcal{D} \\ -i \tilde{\mathcal{E}}^*(t) \mathcal{D} & i \tilde{\mathcal{E}}^*(t) \mathcal{D}^* & -\Delta \tilde{\mathcal{I}}(t) & 0 \\ i \tilde{\mathcal{E}}(t) \mathcal{D}^* & -i \tilde{\mathcal{E}}(t) \mathcal{D} & 0 & -\Delta^* \tilde{\mathcal{I}}(t) \end{pmatrix}. \quad (\text{A12})$$

APPENDIX B: MOMENTS AND CUMULANTS

Let $x(t)$ be a random process dependent on random times t_i , for $i = 1$ to n . Then, an n^{th} -order multitime moment is a kind of averaging defined by the following expression:

$$\begin{aligned} M_n(t_1, t_2, \dots, t_n) & \equiv \langle x(t_1)x(t_2) \cdots x(t_n) \rangle \\ & = \int dx_1 dx_2 \cdots dx_n p_n(x_1, x_2, \dots, x_n) x_1 x_2 \cdots x_n, \end{aligned} \quad (\text{B1})$$

where $p_n(x_1, x_2, \dots, x_n)$ is the n^{th} -order joint *probability density distribution* of the $X(t)$ random process and $x_i = x(t_i)$. Very frequently the physical conditions allow the description in terms of an important class of stochastic processes which require the knowledge of only the first and second moments, $\langle x(t_1) \rangle$ and $\langle x(t_1)x(t_2) \rangle$, i.e., the mean and the autocorrelation (AC) functions, respectively (for radiation field these are known as statistical first and second coherence functions). In such cases we say that the process obeys *Gaussian* statistics.

If $x(t)$ obeys Gaussian statistics the higher-order moments factorize into the products of the first two moments: the mean and the AC function. However, despite this reduction in terms of the lowest two moments, the higher-order moments may still strongly contribute to the system's EOMs. It is here, the multitime cumulant averages (or semi-invariants) enter as an alternative statistical machinery [40]. Cumulants are a particular combination of moments with special properties,

$$C_n(t_1, t_2, \dots, t_n) \equiv \langle x(t_1)x(t_2) \cdots x(t_n) \rangle_c. \quad (\text{B2})$$

The cumulants exhibit what is called a ‘‘cluster’’ behavior in contrast to a ‘‘factorization’’ property of moments for Gaussian processes [Eq. (C9)]. Due to this, all cumulants beyond the second strictly vanish for Gaussian processes whereas for non-Gaussian ones they successively decrease. So, the cumulants have the appropriate behavior to serve a twofold role: First, as successive terms of a perturbative expansion, and second, as a robust measure of the non-Gaussianity of the random field, any cumulant average of higher order beyond the second is exclusively due to the non-Gaussian statistical properties of the process.

In the particular case (and of relevance in the main text) of a zero mean value, $\langle x(t) \rangle = 0$, the cumulants simplify considerably. For simplicity, assuming $x(t)$ as a scalar

random process and using a compact notation for the moments and the cumulants, $M_{ijk\dots n} = M_n(t_i, t_j, \dots, t_n)$ and $C_{ijk\dots n} = C_n(t_i, t_j, \dots, t_n)$, respectively, we have

$$\begin{aligned} C_1 &= 0, \quad C_{12} = M_{12}, \quad C_{123} = M_{123}, \\ C_{1234} &= M_{1234} - M_{12}M_{34} - M_{13}M_{24} - M_{14}M_{23}. \end{aligned} \quad (\text{B3})$$

If, in addition, the $x(t)$ has Gaussian probability distribution all the odd moments vanish ($C_{123} = 0$) while the even ones factorize in terms of the second moments (M_{ij}). For the fourth moment,

$$M_{1234} = M_{12}M_{34} + M_{13}M_{24} + M_{14}M_{23},$$

with the immediate result $C_{1234} = 0$. Therefore for Gaussian processes we are left with the cumulants $C_1 = 0$ and $C_{12} = M_{12}$. The higher cumulants vanish whereas the higher moments are expressed in terms of the second moment M_{ij} , but do not vanish.

APPENDIX C: PARTIALLY ORDERED CUMULANTS

In this Appendix we calculate the first four expansion terms of the averaged equation [Eq. (20)] by explicit calculation of the $\dot{K}(t)$ operator in Eq. (19). Let's consider the average evolution operator $\tilde{U}(t)$ of Eq. (14):

$$\langle \tilde{U}(t) \rangle = \mathbb{1} + \sum_{n=1} U_n(t), \quad (\text{C1})$$

with the $U_n(t)$ terms defined in Eq. (16). The time derivative of $U_n(t)$ is given by

$$\dot{U}_n(t) = \int_{t_i}^t dt_1 \int_{t_i}^{t_1} dt_2 \cdots \int_{t_i}^{t_{n-2}} dt_{n-1} M_n(t, t_1, \dots, t_{n-1}), \quad (\text{C2})$$

with $M_n(t_1, \dots, t_n)$ given in Eq. (B1). The integral limits ensure the prescribed chronological order $t > t_1 > t_2 > \dots > t_n > t_i$. For noncommutative matrices, the chosen evaluation order in the integral matters was taken into consideration by introducing the proper chronological (Dyson) operator in the time derivative of $K(t)$:

$$\begin{aligned} \dot{K}(t) &= \hat{T} \left[\frac{\langle \dot{\tilde{U}}(t) \rangle}{\langle \tilde{U}(t) \rangle} \right] = \hat{T} \left[\frac{\sum_n \dot{U}_n}{\mathbb{1} + \sum_n U_n} \right] \\ &= \hat{T} \left[\left(\sum_n \dot{U}_n \right) \left(\mathbb{1} - \sum_n U_n + \left(\sum_n U_n \right)^2 - \dots \right) \right]. \end{aligned}$$

In the second line of the last equation a Neumann expansion of the denominator was performed. This is a legitimate expansion, provided that $|\sum_n U_n| < 1$, an assumption which should hold if the elements U_n are to be used to make up an evolution operator. Expanding the terms of the last line inside the \hat{T} bracket and gathering together those of the same order we have (up to fourth power are shown below)

$$\begin{aligned} & (\dot{U}_1 + \dot{U}_2 + \dots) (\mathbb{1} - U_1 - U_2 - \dots + U_1^2 + U_2^2 + \dots) \\ &= \dot{U}_1 + \dot{U}_2 + \dot{U}_3 + \dot{U}_4 - \dot{U}_1 U_1 - \dot{U}_1 U_2 - \dot{U}_1 U_3 \\ & \quad - \dot{U}_2 U_1 - \dot{U}_2 U_2 \cdots - \dot{U}_3 U_1 - \dots \\ & \quad + \dot{U}_1 U_1^2 + \dot{U}_1 U_1 U_2 + \dot{U}_1 U_2 U_1 + \dots \\ &= \dot{U}_1 + (\dot{U}_2 - \dot{U}_1 U_1) + (\dot{U}_3 - \dot{U}_1 U_2 - \dot{U}_2 U_1 + \dot{U}_1 U_1^2) \end{aligned}$$

$$\begin{aligned}
 &+ (\dot{U}_4 - \dot{U}_2 U_2 - \dot{U}_1 U_3 - \dot{U}_3 U_1 + \dot{U}_1 U_1 U_2 + \dot{U}_1 U_2 U_1) \\
 &+ \dots + O(U^5).
 \end{aligned}$$

So we may write compactly $\dot{K}(t) = \sum_{n=1}^{\infty} \dot{\kappa}_n(t)$ with

$$\dot{\kappa}_1(t) = \hat{T}[\dot{U}_1] = 0, \quad (\text{C3})$$

$$\begin{aligned}
 \dot{\kappa}_2(t) &= \hat{T}[\dot{U}_2 - \dot{U}_1 U_1] = \hat{T}[\dot{U}_2] \\
 &= \int_{t_i}^t dt_1 M_2(t, t_1), \quad (\text{C4})
 \end{aligned}$$

$$\begin{aligned}
 \dot{\kappa}_3(t) &= \hat{T}[\dot{U}_3 - \dot{U}_1 U_2 - \dot{U}_2 U_1 + \dot{U}_1 U_1^2] = \hat{T}[\dot{U}_3] \\
 &= \int_{t_i}^t dt_1 \int_{t_i}^{t_1} dt_2 M_3(t, t_1, t_2), \quad (\text{C5})
 \end{aligned}$$

where due to our special choice of $\langle \tilde{L}(t) \rangle = 0$ we set $U_1 = \dot{U}_1 = 0$. In addition the chronological operator becomes redundant since the integral limits take care automatically the chosen prescription. For the $\dot{\kappa}_4(t)$ term some further algebra is required though:

$$\begin{aligned}
 \dot{\kappa}_4(t) &= \hat{T}[\dot{U}_4 - \dot{U}_2 U_2] \\
 &= \hat{T} \left[\int_{t_i}^t dt_1 \int_{t_i}^{t_1} dt_2 \int_{t_i}^{t_2} dt_3 M_4(t, t_1, t_2, t_3) \right] - \hat{T} \left[\int_{t_i}^t dt_1 M_2(t, t_1) \int_{t_i}^t dt_2 \int_{t_i}^{t_2} dt_3 M_2(t_2, t_3) \right] \\
 &= \int_{t_i}^t dt_1 \int_{t_i}^{t_1} dt_2 \int_{t_i}^{t_2} dt_3 M_4(t, t_1, t_2, t_3) - \hat{T} \left[\int_{t_i}^t dt_1 \int_{t_i}^t dt_2 \int_{t_i}^{t_2} dt_3 M_2(t, t_1) M_2(t_2, t_3) \right]. \quad (\text{C6})
 \end{aligned}$$

It is not straightforward to drop the \hat{T} operator from the last line since the integral limits do not coincide with the prescribed time ordering $t > t_1 > t_2 > t_3 > t_i$. Some manipulations are needed to arrive at a triple integral with the proper limits. To this end we make use of the following identity:

$$\int_b^a dx \int_x^a dy f(x, y) = \int_b^a dx \int_b^x dy f(y, x). \quad (\text{C7})$$

Adopting temporarily the notation, $M_2(t_i, t_j) = M_{ij}$ and dropping the \hat{T} operator each time that conforms with the integral limits, we have for the last line of Eq. (C6):

$$\begin{aligned}
 &\hat{T} \left[\int_{t_i}^t dt_1 \int_{t_i}^{t_1} dt_2 \int_{t_i}^{t_2} dt_3 M_{01} M_{23} \right] + \hat{T} \left[\int_{t_i}^t dt_1 \int_{t_1}^t dt_2 \int_{t_i}^{t_2} dt_3 M_{01} M_{23} \right] \\
 &= \int_{t_i}^t dt_1 \int_{t_i}^{t_1} dt_2 \int_{t_i}^{t_2} dt_3 M_{01} M_{23} + \hat{T} \left[\int_{t_i}^t dt_1 \int_{t_1}^t dt_2 \int_{t_i}^{t_1} dt_3 M_{01} M_{23} \right] + \hat{T} \left[\int_{t_i}^t dt_1 \int_{t_1}^t dt_2 \int_{t_1}^{t_2} dt_3 M_{01} M_{23} \right] \\
 &= \int_{t_i}^t dt_1 \int_{t_i}^{t_1} dt_2 \int_{t_i}^{t_2} dt_3 M_{01} M_{23} + \int_{t_i}^t dt_1 \int_{t_i}^{t_1} dt_2 \int_{t_i}^{t_2} dt_3 M_{02} M_{13} + \hat{T} \left[\int_{t_i}^t dt_1 \int_{t_i}^{t_1} dt_2 \int_{t_2}^{t_1} dt_3 M_{02} M_{13} \right] \\
 &= \int_{t_i}^t dt_1 \int_{t_i}^{t_1} dt_2 \int_{t_i}^{t_2} dt_3 M_{01} M_{23} + \int_{t_i}^t dt_1 \int_{t_i}^{t_1} dt_2 \int_{t_i}^{t_2} dt_3 M_{01} M_{23} + \int_{t_i}^t dt_1 \int_{t_i}^{t_1} dt_2 \int_{t_1}^{t_2} dt_3 M_{03} M_{12}.
 \end{aligned}$$

Now we can replace the integral of Eq. (C6) and arrive at the final expression:

$$\dot{\kappa}_4(t) = \int_{t_i}^t dt_1 \int_{t_i}^{t_1} dt_2 \int_{t_i}^{t_2} dt_3 [M_4(t, t_1, t_2, t_3) - M_2(t, t_1) M_2(t_2, t_3) - M_2(t, t_2) M_2(t_1, t_3) - M_2(t, t_3) M_2(t_1, t_2)]. \quad (\text{C8})$$

Note that for stochastic fields with Gaussian statistics and in the case of commutative matrices, we would have $\dot{\kappa}_3 = \dot{\kappa}_4 = 0$ if we take into account the properties of the nonvanishing multitime moments [25]:

$$M_{ijkl\dots mn} = \sum M_{i'j'} M_{k'l'} \dots M_{m'n'}, \quad n \text{ even} \quad (\text{C9})$$

where $(i', j'), (k', l'), \dots (m', n')$ pairs are all possible combinations of the indices $(i, j, k, l, \dots, m, n)$.

One may continue and work out the higher-order cumulant expressions along similar lines if they are needed. Nevertheless, alternative recipes (not less laborious, though) for their calculations in terms of the moments may also be found in the original literature [25,40].

[1] H. Wabnitz, L. Bittner, A. R. B. de Castro, R. Dohrmann, P. Gurtler, T. Laarmann, W. Laasch, J. Schulz, A. Swiderski, K. von Haefen, T. Möller, B. Faatz, A. Fateev, J. Feldhaus, G.

Gerth, U. Hahn, E. Saldin, E. Schneidmiller, K. Sytchev, K. Tiedke, R. Treusch, and M. Yorkov, *Nature (London)* **420**, 482 (2002).

- [2] W. Ackermann, G. Asova, V. Ayzvazyan, A. Azima, N. Baboi, J. Bahr, V. Balandin, B. Beutner, A. Brandt, A. Boltzmann *et al.*, *Nat. Photon.* **1**, 336 (2007).
- [3] L. Young, E. P. Kanter, B. Krässig, Y. Li, A. M. March, S. T. Pratt, R. Santra, S. H. Southworth, N. Rohringer, L. F. DiMauro, G. Doumy, C. A. Roedig, N. Berrah, L. Fang, M. Hoener, P. H. Bucksbaum, J. P. Cryan, S. Ghimire, J. M. Glowina, D. A. Reis, J. D. Bozek, C. Bostedt, and M. Messerschmidt, *Nature (London)* **466**, 56 (2010).
- [4] N. V. Kampen, *Phys. Rep.* **24**, 171 (1976).
- [5] A. Papoulis and S. U. Pilai, *Probability, Random Variables and Stochastic Processes* (McGraw-Hill, New York, 2002).
- [6] M. Lax, W. Cai, and M. Xu, *Random Processes in Physics and Finance* (Oxford University Press, Oxford, 2006).
- [7] G. S. Agarwal, *Phys. Rev. A* **1**, 1445 (1970).
- [8] A. T. Georges and P. Lambropoulos, *Phys. Rev. A* **20**, 991 (1979).
- [9] P. Zoller, *J. Phys. B* **15**, 2911 (1982).
- [10] J. H. Eberly, K. Wódkiewicz, and B. W. Shore, *Phys. Rev. A* **30**, 2381 (1984).
- [11] N. Rohringer and R. Santra, *Phys. Rev. A* **77**, 053404 (2008).
- [12] L. A. A. Nikolopoulos, T. J. Kelly, and J. T. Costello, *Phys. Rev. A* **84**, 063419 (2011).
- [13] D. Middleton and L. A. A. Nikolopoulos, *J. Mod. Opt.* **59**, 1650 (2012).
- [14] G. M. Nikolopoulos and P. Lambropoulos, *Phys. Rev. A* **86**, 033420 (2012).
- [15] G. Mouloudakis and P. Lambropoulos, *Eur. Phys. J. D* **72**, 226 (2018).
- [16] N. A. Papadogiannis, L. A. A. Nikolopoulos, D. Charalambidis, G. D. Tsakiris, P. Tzallas, and K. Witte, *Appl. Phys. B* **76**, 721 (2003).
- [17] S. Krinsky and Y. Li, *Phys. Rev. E* **73**, 066501 (2006).
- [18] S. O. Rice, *Bell Syst. Tech. J.* **23**, 282 (1944).
- [19] M. Y. Evgeny Saldin and E. V. Schneidmiller, *The Physics of Free Electron Lasers* (Springer-Verlag, Berlin, Heidelberg, 2000).
- [20] K.-J. Kim, Z. Huang, and R. Lindberg, *Synchrotron Radiation and Free-Electron Lasers*, 1st ed. (Cambridge University Press, Cambridge, 2017).
- [21] J. W. Goodman, *Statistical Optics* (John Wiley and Sons, New York, 1985).
- [22] N. Wax, *Selected Papers on Noise and Stochastic Processes* (Dover Publications, Mineola, 1954).
- [23] R. F. Fox, *Phys. Rep.* **48**, 179 (1978).
- [24] C. W. Gardiner, *Handbook of Stochastic Methods for Physics, Chemistry and the Natural Sciences* (Springer-Verlag, Berlin, Heidelberg, 1954).
- [25] N. V. Kampen, *Stochastic Processes in Physics and Chemistry* (Elsevier Science, Amsterdam, 1992).
- [26] V. Shapiro and V. Loginov, *Physica A* **91**, 563 (1976).
- [27] M. Schubert and B. Wilhelmi, *Nonlinear Optics and Quantum Electronics* (Wiley-Interscience, New York, 1986).
- [28] P. Avan and C. Cohen-Tannoudji, *J. Phys. B* **10**, 155 (1977).
- [29] U. Fano, *Phys. Rev.* **124**, 1866 (1961).
- [30] P. Lambropoulos and P. Zoller, *Phys. Rev. A* **24**, 379 (1981).
- [31] L. A. A. Nikolopoulos, T. Nakajima, and P. Lambropoulos, *Eur. Phys. J. D.* **20**, 297 (2002).
- [32] D. T. Haar, *Rep. Prog. Phys.* **24**, 304 (1961).
- [33] L. Mandel and E. Wolf, *Optical Coherence and Quantum Optics* (Cambridge University Press, Cambridge, 1995).
- [34] S. Krinsky and R. L. Gluckstern, *Phys. Rev. ST Accel. Beams* **6**, 050701 (2003).
- [35] K. Blum, *Density Matrix Theory and Applications*, 3rd ed. (Springer-Verlag, Berlin, Heidelberg, 2012).
- [36] L. A. A. Nikolopoulos, *Elements of Photoionization Quantum Dynamics Methods* (Morgan & Claypool Publishers, San Rafael, 2019).
- [37] A. T. Georges and P. Lambropoulos, *Advances in Electronics and Electron Physics* (Academic Press, New York, 1980), Vol. 54.
- [38] L. A. A. Nikolopoulos, T. Nakajima, and P. Lambropoulos, *Phys. Rev. Lett.* **90**, 043003 (2003).
- [39] C. Cohen-Tannoudji, J. Dupont-Roc, and G. Grynberg, *Atom-Photon Interactions, Basic Processes and Applications* (John Wiley and Sons, New York, 1977).
- [40] R. Kubo, *J. Phys. Soc. Jpn.* **17**, 1100 (1962).
- [41] L. Nikolopoulos, *Comput. Phys. Commun.* **150**, 140 (2003).
- [42] L. A. A. Nikolopoulos and P. Lambropoulos, *New J. Phys.* **10**, 025012 (2008).
- [43] J. M. Rost, K. Schulz, M. Domke, and G. Kaindl, *J. Phys. B: At. Mol. Opt. Phys.* **30**, 4663 (1997).
- [44] S. Schippers, *J. Quant. Spectro. Radia. Trans.* **219**, 33 (2018).
- [45] C. Ott, L. Aufleger, T. Ding, M. Rebholz, A. Magunia, M. Hartmann, V. Stooß, D. Wachs, P. Birk, G. D. Borisova, K. Meyer, P. Rupprecht, C. da Costa Castanheira, R. Moshhammer, A. R. Attar, T. Gaumnitz, Z.-H. Loh, S. Düsterer, R. Treusch, J. Ullrich, Y. Jiang, M. Meyer, P. Lambropoulos, and T. Pfeifer, *Phys. Rev. Lett.* **123**, 163201 (2019).
- [46] S. Nakajima, *Prog. Theor. Phys.* **20**, 948 (1958).
- [47] R. Zwanzig, *J. Chem. Phys.* **33**, 1338 (1960).